JOURNAL OF OPTOELECTRONICS AND ADVANCED MATERIALS Vol. 12, No. 2, February 2010, p. 301 - 308

# Fracture toughness of alumina matrix composites (AMC)

M. SZUTKOWSKA[a,b], M. BONIECKI[c]
[a]*The Institute of Advanced Manufacturing Technology, Cracow 30011, Poland,*
[b]*Pedagogical University of Cracow, Cracow 30084, Poland*
[c]*The Institute of Electronic Materials Technology, Warsaw 01919, Poland*

YSZ solid electrolyte with high fracture toughness as well as enhanced strength is required from a performance and structural reliability point of view. A specific characteristic in fracture toughness measurement according to various methods of advanced alumina matrix composites with particular reference to $Al_2O_3$-$ZrO_2$ composites is a main goal of the presentation. The values of the $K_{IC}$ obtained by conventional method on the mechanically notched specimen type SENB (Single Edge Notched Beam) were compared with indentation fracture toughness. Indentation fracture toughness has been determined from direct measurement of the crack length, developed during the Vickers indentation test. The modified method of direct crack measurement has also been used for determination of the fracture toughness. The parameters of subcritical crack growth were determined. Chipping compliance of the alumina matrix composites under different loads applied to the Vickers hardness indenter was tested. The composites $Al_2O_3$-10 wt.% $ZrO_2$ with unstabilised $ZrO_2$, yttria or ceria stabilized $ZrO_2$ were tested.

(Received February 20, 2009; accepted February 18, 2010)

*Keywords:* Fracture toughness, Indentation fracture toughness, Subcritical crack growth, Ceramic matrix composites.

## 1. Introduction

Solid oxide fuel cells (SOFC) are currently being developed for various power generation applications. The major components of a SOFC are the electrolyte, the anode, the cathode, and the interconnection. The two porous electrodes, anode and cathode, are separated by a fully dense solid electrolyte. Currently, yttria-stabilized zirconia (YSZ) is the most commonly used electrolyte in SOFC because of its highoxygen ion conductivity, stability in both oxidizing and reducing environments, availability, and low cost. Fracture in the solid oxide electrolyte will allow the fuel and oxidant to come in contact with each other resulting in reduced cell efficiency or in some cases malfunction of the SOFC. Therefore, YSZ solid electrolyte with high fracture toughness as well as enhanced strength is required from a performance and structural reliability point of view. Furthermore, because of high operating temperature (around 1000 °C) in SOFCs, it is certainly expected that slow crack growth would take place, which limits the life of electrolyte or SOFC system [1]. Therefore, it is important to determine slow crack growth or life prediction parameters of the material to ensure accurate life prediction of SOFC components. The significant problem concerning solid oxide fuel cells is using electrolyte working in the range of intermediate temperatures up to 800°C (IT – SOFC), which would provide stable electrical conductivity at the fuel cell operating temperature as well as it would exhibit relatively high mechanical properties.

Ceramic matrix composites (CMCs) combine reinforcing ceramic phases with a ceramic matrix to create materials with new and superior properties. In ceramic matrix composites, the primary goal of the ceramic reinforcement is to provide toughness to an otherwise brittle ceramic matrix. The desirable characteristics of CMCs include high-temperature stability, high thermal shock resistance, high hardness, high corrosion resistance, light weight, nonmagnetic, nonconductive properties, sufficient levels of strength and fracture toughness and versatility in providing unique engineering solutions. The combination of these characteristics makes ceramic matrix composites attractive alternatives to traditional processing industrial materials such as high alloy steels and refractory metals. For the processing industry, related benefits of using ceramic composites include increased energy efficiency, increased productivity, and regulatory compliance. Some of the more common oxide matrices include alumina, silica, mullite, barium aluminosilicate, lithium aluminosilicate and calcium aluminosilicate. Of these, alumina and mullite have been the most widely used because of their in-service thermal and chemical stability and their compatibility with common reinforcements. The drawback of ceramics in comparison with metals is their extremely low fracture-toughness. It means that ceramics have a very low tolerance of crack-like flaws. The absence of energy-dissipating mechanisms, such as generation and movement of dislocations in ceramics, causes ceramics to fail in a catastrophic fashion. Improving the toughness of ceramics is the current research goal. One of the important approaches to accomplish this goal is via ceramic matrix composites. Fracture of ceramics often starts from cracks, which may originate at pores and inclusions or may be generated during surface treatment. Various failure modes are responsible for failure and finite lifetime of ceramic materials. At moderate temperatures the most important of them are: spontaneous failure, subcritical crack growth (sometimes called slow-crack-growth) under static load,

cyclic fatigue, thermal shock and thermal fatigue [2]. The failure of ceramics can be caused by subcritical crack growth of preexisting flaws until their critical dimension is attained. The subcritical crack growth (SCG) is a time-dependent phenomenon, where a crack is growing at a load below $K_I=K_{Ic}$ (where: $K_I$ is a stress intensity factor but $K_{Ic}$ is the fracture toughness). Crack growth is governed only by the stress intensity factor $K_I$ and for a given material and environment there is an unique relation between the crack growth velocity v and $K_I$ [3]:

$$v = \frac{dc}{dt} = f(K_I) \tag{1}$$

In Fig.1 the crack velocity (v) versus stress intensity factor ($K_I$) curve is shown in the log-log representation.

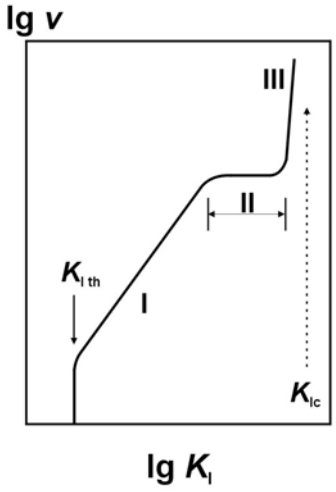


*Fig.1. Typical v-$K_I$ curve.*

In case of ideally brittle materials the fracture toughness is independent of the crack extension and, consequently, identical with the stress intensity factor $K_{I0}$ necessary for the onset of stable crack growth. The threshold $K_{I0}$ in the stress-intensity factor under which no crack propagation occurs specifies a safety range of use for structural application. At low crack growth velocities an extended range occurs with straight line in the crack velocity (v) versus stress intensity factor ($K_I$) curve . In this region the crack growth velocity fulfills a power-law relation (2):

$$v = A K_I^n = A^* \left[ \frac{K_I}{K_{IC}} \right]^n \tag{2}$$

with the proportionality constants *A, A** and an empirical parameter *n* depending on the material, the temperature and the environment [4]. The high value of *n* (>50) was observed for most ceramics in dry or inert (Ar) conditions, but for most oxide ceramics in water containing environments the low values of *n* are determined. In some case threshold value $K_{I0}$ can be detected, below which no subcritical crack growth is found [5].

The fracture toughness for ceramic matrix composites is one of the most controversial issues in materials testing, with more than 30 different tests and many variations for each test [6]. A bewildering number of specimen geometries and experimental methods has been proposal (and adopted) to determine the fracture toughness of CMCs. However up to now, no universally agreed standard for fracture toughness exists. In spite of long-lasting works carried by the technical committee ISO/TC119 none of the methods for the measurement of fracture toughness for ceramics are internationally standardized. Considering a various approach to determine the fracture toughness several significance of this term has been used as: plane strain fracture toughness $K_{IC,}$ strain energy release rate $G_{IC}$, indentation fracture toughness (sometime termed Vickers/Palmqvist toughness). The most accepted methods specify a precracked specimen loaded to fracture under three point bending (3PB) – so called conventional methods. The conventional methods of fracture toughness determination realized at the three point bending test (3PB) with notched beams require of complex testing procedure and using specimens with greater dimensions and complicate geometry. It increases a cost and labour consumption of the test. Mentioned difficulties become inspiration to working out alternative method of fracture toughness measurement by means of a point indentation technique. In this method Vickers hardness indenter to induce cracks in the CMCs is used. A high fracture toughness of the structural materials is considered to be an essential property to achieve safety and integrity.

## 2. Experimental procedures

Different types of alumina matrix composites were used in this study like: alumina-10 wt% zirconia composite with nano 12 mol% $CeO_2$ stabilized $ZrO_2$, alumina-10 wt% zirconia composite with unstabilized $ZrO_2$, alumina-10 wt% zirconia composite with 3%mol $Y_2O_3$ stabilized $ZrO_2$. A high purity alumina powder $\alpha$-$Al_2O_3$ > 99.8 wt% type A16SG produced by the Alcoa firm with an average particle size of below 0.5 μm and nano ceria stabilized zirconia CEZ-12 Daiichi Kicenso Kogyo Co LTD were used to process ceramics samples. The pure zirconia was obtained by precipitation from water solution of $ZrOCl_2$ by means of water solution of ammonia. Sintering additives, such the MgO to inhibit grain growth have been introduced. Specific surface areas $S_{BET}$=4.54 $m^2/g$ of the alumina particles, pure zirconia $S_{BET}$=41.3 $m^2/g$, and 3mol% yttria doped zirconia, $S_{BET}$=4.70 $m^2/g$ respectively were measured by the BET multipoint method, using $N_2$ as the adsorption/desorption gas at the temperature of liquid nitrogen. Agglomerate of the zirconia stabilized with 12 mol% $CeO_2$ particles with BET surface areas approximately $S_{BET}$=10.7 $m^2/g$ and average size of 0.4 μm was disintegrated. Solid solution of 3 mol% yttria doped zirconia has been obtained by co-precipitation from the common aqueous solution of the

$ZrOCl_2$ +$YCl_3$. Processing steps included die pressing the powder at 50 MPa, is pressing at 250 MPa, and sintering in air for 2 h at 1923 K. Conventional methods and indentation technique were used for determination of the fracture toughness.

### 2.1 Conventional methods

A variety of testing methodologies exist, and the most widely and favorably used are single-edge-precracked-beam (SEPB), double torsion (DT), double notched beam DCB and chevron-notched-beam (CVNB) methods. The specimen produces the sharp crack during loading. The main advantage of specimens with chevron notches (see Fig. 2) is the fact that no sharp precrack has to be introduced.

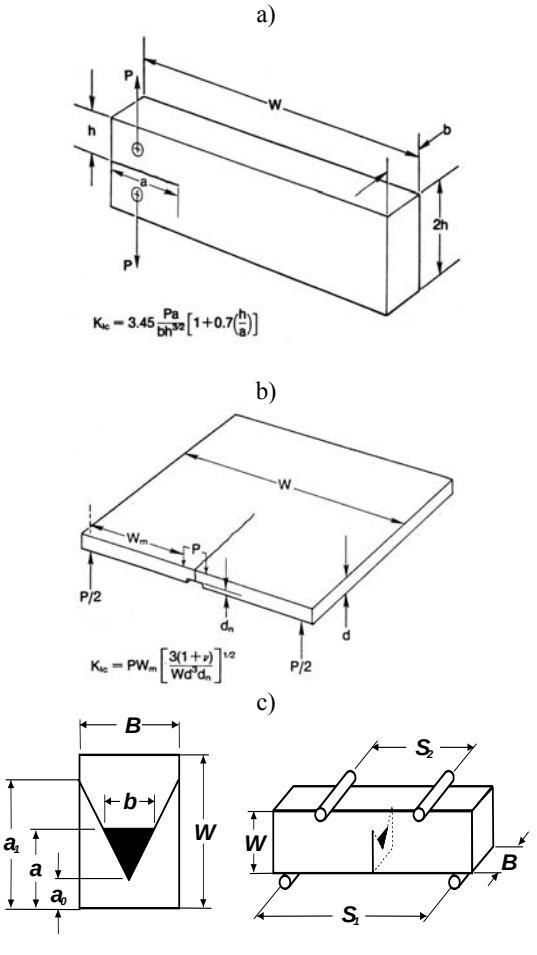


*Fig. 2. Different kind of specimen used in fracture toughness test : a) Double Torsion (DT), b) Double Cantilever Beam (DCB), c) Chevron Notched Beam (CVNB) for a four-point bending.*

The procedure for a measurement of fracture toughness is based essentially on the principle of linear-elastic fracture mechanics (LEFM) and it includes three main steps: the generation of cracks in the test specimen, the measurement of a load at failure stress respectively, and the crack depth. The single edge notch beam (SENB) specimen with sharp notch precracked in mechanical impact or fatigue way loaded to fracture with 3PB is widely accepted. Short rod or bar specimen with chevron-shaped slot to determine of the fracture toughness $K_{ICSR}$ is recommended as well. Load versus displacement across the slot at the specimen mouth is recorded autographically. As a load test machine, fractometer a trademark of Terra Tek systems has been found satisfactory for this purpose. The generation of a reproducible sharp and accurately positioned precrack in ceramic matrix composites gives from the technical point of view a problem. It partially causes the variability of the reported fracture toughness results. In practice a thin notch (typically about 100 μm) is cut using a diamond cutting disk.

The mechanical test conducted in this study included three–point bending test up to failure. The SENB specimens thinned out to the size 1.5 × 4.0 × 50.0 ±0.1mm with wide polished side surface and vacuum evaporated thin aluminium layer (about 150 nm thick) were mechanically notched. These specimens with an initial 0.9 mm length of notch produced by diamond saw (0.20 mm thick) prior to testing were precracked by thin diamond saw (0.025 mm thick) so that the total initial crack length was approximately 1.1 mm (Fig.3).

Relationship of $K_{IC} = f(c)$ is given by equation (3,4) [7]:

$$K_{IC} = 1.5\frac{P_c S}{W^2 B} Yc^{1/2} \tag{3}$$

$$Y = \frac{\sqrt{\Pi}}{(1-\beta)^{\frac{3}{2}}}\left[0.3738\beta + (1-\beta)\sum_{i,j=0}^{4} A_{ij}\beta^i\left(\frac{W}{S}\right)^j\right] \tag{4}$$

where: $P_c$ is the critical load, $S$ is the support span, $W$ is the width, $B$ is the specimen thickness, $Y$ is the geometric function, $c$ is the crack length, $\beta$ is the c/W and $A_{ij}$ are the coefficients given by Fett [7].

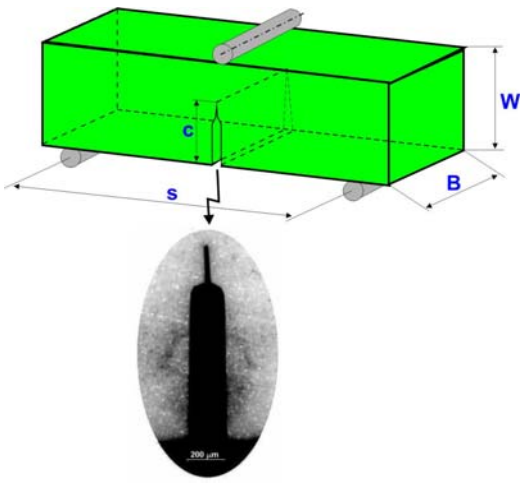


*Fig.3. SENB specimen with the notch view*

### 2.2. Indentation fracture toughness

Indentation technique long has been considered an attractive method for assessing the toughness of ceramics because of the ease and low cost of conducting experiments. Considering a various approach to determine the fracture toughness of alumina matrix composites a greater attention was paid on the indentation methods. Now there are a very large number of theoretical models in the literature relating the surface cracks measured after indentation to the Vickers indenter load and material parameters. Such cracks emanate from the indent as a result of residual tensile stresses that develop during unloading. Relationship between loading force of indenter and crack length is linear. It is empirical relationship without theoretical substructure but indicating close correlation with mechanical properties of tested materials. As a result of hardness indenter indentation at the ceramic matrix composites surface a plastic zone beneath the indent is originated according to elastic-plastic mode. Due to effect of the plastic deformation zone with surrounding its elastic matrix in the ceramics the crack system is generated.

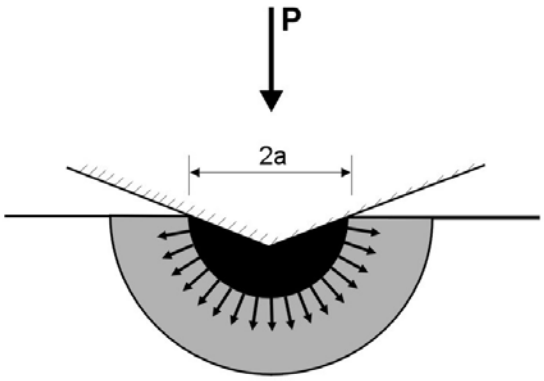


*Fig.4. Model of elastic-plastic Vickers indentation. Dark region denotes "hydrostatic core", shaded region presents "plastic zone", and surrounding region is "elastic matrix". [8]*

Four microcrack morphologies develop in ceramic matrix composites. Median cracks, radial cracks (a half-penny shaped elliptical crack, much larger than the median crack), lateral cracks (in a plane normal to the median and radial cracks) and Palmqvist radial cracks (originating near the edge of the plastic zone beneath the indent) are observed in ceramics (Fig.5).

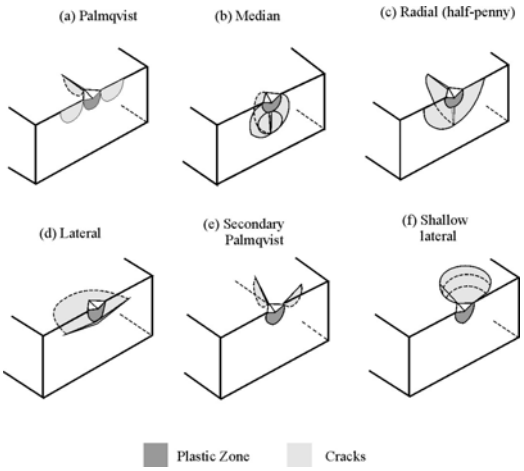


*Fig.5. Primary (a,b,c,d) and secondary (e,f) crack systems produced by the Vickers hardness indentation in ceramics [4].*

There is still considerable debate regarding the nature of the cracks observed around the Vickers indentation. The most commonly used crack systems produced by the Vickers hardness indenter show Figures 5a to 5d. The Palmqvist cracks form at apexes of the indentation impression remaining connected to the surface. Median cracks are generated beneath the indentation impression (Fig.5b). They are in the shape of a penny and lie on a plane of symmetry containing the contact axis. Upon complete removal of the indenter, the radial and median cracks sometimes meet to form half-penny cracks (Fig. 5c). During unloading at high indentation loads, lateral cracks (Fig.5d) may nucleate beneath the indenter and propagate sideways in a circular form, which may divert upwards towards the surface and cause chipping. In addition to the above commonly observed crack systems, other variant crack systems could also be produced by the Vickers indentation. They include secondary Palmqvist cracks (Fig.5e) and shallow lateral cracks (Fig.5f), which emanate from the edge of the indentation impression in some cases.

Both the Palmqvist and median/radial cracks emanating from the corner of the Vickers hardness indentation provide base to determination the indentation fracture toughness. In any indentation fracture toughness determination a critical stress intensity factor is a proper accounting of the residual contact stresses in the fracture mechanics formulas. These stresses play primary role in driving the cracks at all stages of growth, both during and after the indentation cycle. A correlation between the fracture toughness and ratio of cracks to indent size expressed according to selected equations proposed by different authors: Lankford [9], Niihara [10], Laugier [11], Anstsis [12], Liang [13] and Lawn [14] is presented in Table 1..

*Table1. Selected formulae used for calculation of indentation fracture toughness.*

| Number | Author | Formulas used for calculation of $K_{IC}$ [MPa $m^{1/2}$] Median/radial cracks | Palmqvist cracks |
|---|---|---|---|
| 5 | Niihara et al.[10] | $K_{IC} = 0.129(Ha^{1/2}) ( E\phi /H)^{0.4} (c/a)^{-1.5}/\phi$ | - |
| 6 | Anstis et al.[12] | $K_{IC} = 0.016 ( E/H)^{0.5} (P/c^{3/2})$ | - |
| 7 | Lawn et al. [14] | $K_{IC} = 0.028 ( Ha^{1/2}) (E/H)^{0.5} (c/a)^{-1.5}$ | - |
| 8 | Niihara et al.[10] | | $K_{IC} = 0.035 (Ha^{1/2}) ( E\phi /H)^{0.4} (l/a)^{0.5}/\phi$ |
| 9 | Lankford [9] | | $K_{IC} = 0.142 (Ha^{1/2}) ( E\phi /H)^{0.4} (c/a)^{-1.56}/\phi$ |
| 10 | Laugier [11] | $K_{IC} = 0.010 (E/H)^{2/3} P/c^{3/2}$ | |
| 11 | Laugier [11] | | $K_{IC} = 0.015 (l/a)^{-1/2} (E/H)^{2/3} P/c^{1/2}$ |
| 12 | Liang [13] | $K_{IC} = (Ha^{1/2}) ( E\phi /H)^{0.4} (c/a)^{(c/18a)-1.51}/ \alpha\phi$ $\alpha = 14[ 1-8 (4\nu-0.5/1+\nu)^4 ]$ | |

where: P is the loading force applied to Vickers indenter; l is the crack length; E is the Young's modulus; H, a, ϕ, c, ν are given in equation (1)

### 2.3. Slow-crack-growth (SCG) behavior of alumina matrix composites

For the CMCs under conditions of subcritical crack growth, finite lifetime has to be expected. When simple crack growth relation (2) can be applied, the lifetime can be computed analytically.The relation between crack growth velocity and stress intensity factor can be determined by applying a load to specimens with macrocracks and measuring the crack growth directly or indirectly from the change of the specimen compliance. In presented work, a load-relaxation technique method was used for the observation of a subcritical crack growth. The crack length was evaluated by linear-elastic analysis from the compliance of single-edge-notched specimen (SENB) in three-point bending test.

## 3. Results and discussion

The critical stress intensity factor $K_{IC}$ of tested alumina matrix composites: alumina-zirconia composite with 10%-wt. nonstabilized $ZrO_2$, alumina-10 wt% zirconia composite with nano 12 mol% $CeO_2$ stabilized $ZrO_2$, alumina-10 wt% zirconia composite with 3%mol $Y_2O_3$ stabilized $ZrO_2$.determined on the basis conventional method are presented in Table 2.

*Table 2. $K_{IC}$ values obtained by means of conventional method.*

| Materials | Loading force $F$ [N] | Bending stress $\sigma$ [MPa] | Critical stress intensity factor $K_{IC}$ [MPa $\sqrt{m}$] |
|---|---|---|---|
| | | | |
| $Al_2O_3$-10% masy $ZrO_2$ | 30.3 | 74,9 (1,6)* | 4,68 (0,09)* |
| $Al_2O_3$-10% masy $ZrO_{2(Y2O3)}$ | 30.4 | 76,6 (2,7) | 4,00 (0,16) |
| $Al_2O_3$-10% masy $ZrO_{2(CeO2)}$ | 26.5 | 63.8 (1.7) | 3.96 (0,08) |

where: * standard deviation

The indentation fracture toughness test were used for the same types of alumina matrix composites as for the conventional method. The specimens with dimensions 2.5×4.0×25.0 were tested. The measurements of the indentation fracture toughness at different loads of the Vickers hardness indenter, starting from 9.81 N; 49.5 N; 98.1 N; 294.3 N; 495.0 N up to 981.0 N were carried. On the basis of an own experience [13], fracture toughness $K_{IC}$ calculated from Niihara's equation (4) was used for comparison. In this case, relation between the fracture toughness and the ratio of cracks to indent size at the condition $c/a \geq 2.5$ is expressed by the equation (4):

$$(K_{IC}\, \varphi /H\, a^{1/2}) (H/E\, \varphi)^{2/5} = 0.129\, (c/a)^{-3/2} \qquad (4)$$

where: $K_{IC}$ is the critical stress intensity factor, φ is the constrain factor, H is the Vickers hardness, E is the Young's modulus, a-half of indent diagonal.

Using the expression developed by Niihara et al.[11] normalized fracture curves of $(K_{IC}\phi/Ha^{1/2})$ $(H/E\phi)^{2/5}$ against c/a (Fig.7) were obtained. This relationship exhibits a linear decreasing character. $K_{IC}$ was measured by conventional method (SENB specimens) [12]. The slope of all curves is defined by a parameter ($-m \approx 1.5$) which is a function of the ratio c/a. Ratio of c/a is approached to 2.5 at the lowest loading force 9.81N and increases up to value more than 5 at the loading force 490,5N. The crack profile can change from Palmqvist type at the small c/a ratio<2.5 to median/radial at the ratio c/a >2.5. Mostly observed cracks of tested ceramics have median/radial profile. The lowest value of ratio c/a beneath 2.5 occurs in $Al_2O_3$-10wt% $ZrO_2$ composite what suggest appearance of Palmqvist cracks.

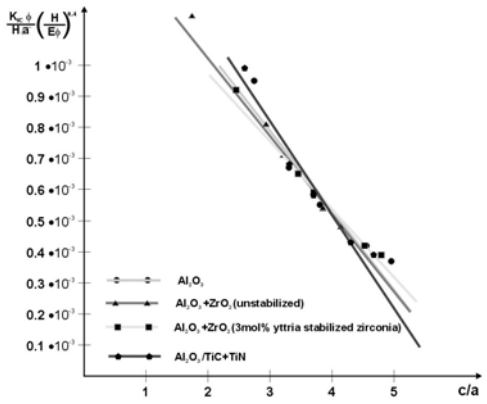


*Fig. 6. Normalized fracture curves of $(K_{IC}\phi/Ha^{1/2})$ $(H/E\phi)^{2/5}$ against c/a for tested ceramics.*

The shallow lateral cracks can 'pop-in' parallel to the surface and terminate subsequently at the surface to remove a flake of ceramics. For the alumina matrix composites shallow lateral cracks without chipping are only visible at indentation load 981.0 N (Fig. 7).

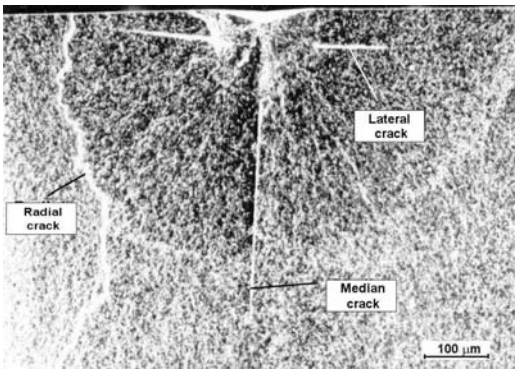


a

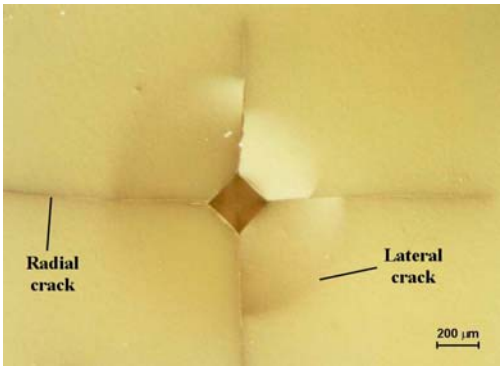


b

*Fig. 7. SEM image of the median/radial and lateral cracks: a) on the fracture surface of the $Al_2O_3$-10 wt% $ZrO_2$ (3 mol% $Y_2O_3$) stabilized $ZrO_2$ at P=294N, b) on the top surface of the $Al_2O_3$-10 wt% $ZrO_2$ (with unstabilized zirconia) at 981N.*

Summary of the indentation fracture toughness $K_{IC}$, determined according to selected formulae, presented by various authors [7-12], are shown in Figure 9.

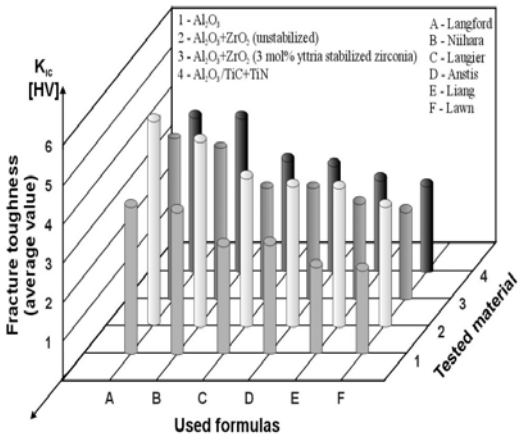


*Fig. 8. Summary of the indentation fracture toughness $K_{IC}$ determined according to selected formulae presented by various authors [7-12].*

As shown in Figure 5 the obtained results indicate strong dependence of the $K_{IC}$ on the formulae accepted for calculations. The difference between the lowest and highest value of $K_{IC}$ is about 50%. The highest value of $K_{IC}$ is calculated using the Lankford's [7] 'universal' equation and is applied regardless of the cracks type, while the lowest value of $K_{IC}$ is for the Lawn's [12] equation. The nearest to conventional fracture toughness (SENB specimen) is $K_{IC}$ determined by equation (4) [13]. The $K_{IC}$ values, obtained by the presented indentation methods, are comparable. The alumina-10 wt% zirconia with unstabilized zirconia composite indicates the highest value of the fracture toughness independently on the used methods. For this composite the difference ranges within 10%-20% for individual tested methods. Relation of in-plane displacements and strain distribution in proximity of Vickers hardness indentation at loading force 98.1 N, and cracks with the $K_{IC}$, was analysed by means of the interferometry method. Examples of the in-plane displacement and strain in v(x,y) plane are shown on displacements and strain contour maps and 3D plots of displacement and strain for the $Al_2O_3$-10 wt% $ZrO_2$ with unstabilized zirconia composite (Fig.9, Fig.10).

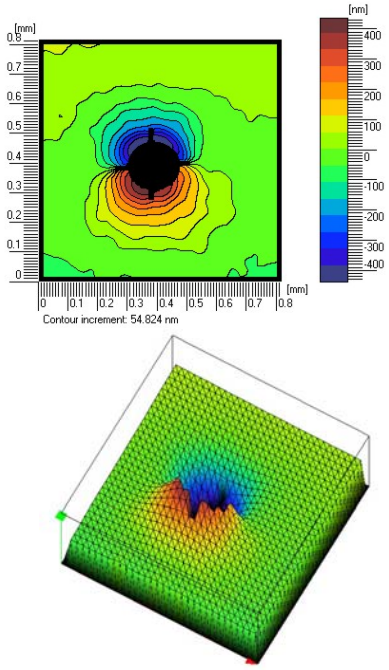


*Fig. 9. The analysis of v(x,y) in-plane displacement nearby Vickers indentation for the $Al_2O_3$-10 wt% $ZrO_2$ with unstabilized zirconia composite: a) contour map, b) 3D map of displacement distribution.*

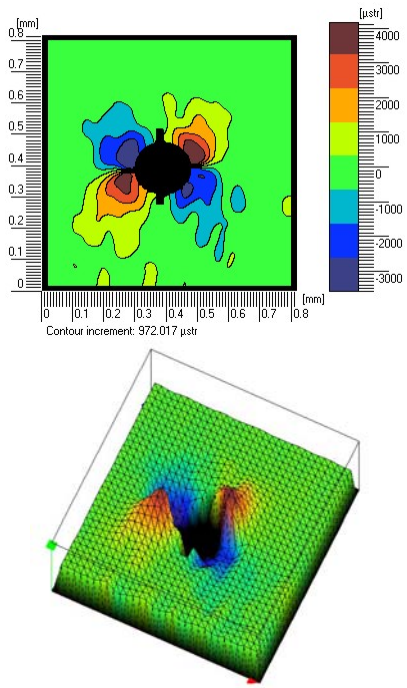


*Fig.10. The analysis of in-plane dv/dx strain representing v(x,y) plane nearby Vickers indentation for the $Al_2O_3$-10 wt% $ZrO_2$ with unstabilized zirconia composite: a) contour map, b) 3D map of strain distribution.*

The in-plane displacements u(x,y) and v(x,y) achieve values placed within the range from 300 nm to 600 nm and their distribution is similar in both directions (Fig.9). Analysis of du/dx and dv/dx strains allows to observe distinct strain concentration at the end of the cracks (Fig.10).

Subcritical crack growth empirical parameter *n* and proportionality constant *logA*, fracture of work *WOF*, stress intensity factor for crack initiation $K_{I0}$, maximum stress intensity factor $K_{Imax}$ determined for the tested ceramics were presented in

*Table 1. Subcritical crack growth parameters (n and, logA), fracture work WOF, stress intensity factor for crack initiation $K_{I0}$, maximum stress intensity factor $K_{Imax}$ determined for the tested ceramics*

| Material | Fracture work, *WOF* ($J/m^2$) | Stress intensity factor for crack initiation, $K_{I0}$ ($MPa\ m^{1/2}$) | *n* Parameter in formula (2) for region* $I(v_a),II(v_b),III(v_c)$ | *logA* Proportionality constant in formula (2) for region $I(v_a),II(v_b),III(v_c)$ | Maximum stress intensity factor, $K_{Imax}$ ($MPa\ m^{1/2}$) |
|---|---|---|---|---|---|
| $Al_2O_3$–10 wt % $ZrO_{2(nano)}$ with nano 12 mol% $CeO_2$ stabilized $ZrO_2$ | 23.5±5.2 | 3.21±0.04 | 20.27 ($v_a$)<br>5.87 ($v_b$)<br>50.75 ($v_c$) | -16.33 ($v_a$)<br>-8.40 ($v_b$)<br>-37.64 ($v_c$) | 5.08±0.09 |
| $Al_2O_3$–10 wt % $ZrO_2$ with unstabilized $ZrO_2$ | 33.4±0.9 | 3.94±0.13 | 19.53 ($v_a$)<br>8.64 ($v_b$) | -18.04 ($v_a$)<br>-10.67 ($v_b$) | 5.51±0.08 |

*Values for *n* and *logA* are calculated for the three region ( see Fig. 1)

The $Al_2O_3$–10 wt% $ZrO_2$ with unstabilized $ZrO_2$ ceramics reveals higher value of $K_{I0}$, $K_{Imax}$ and *WOF* than $Al_2O_3$–10 wt% $ZrO_{2(nano)}$ (12 mol% $CeO_2$) ceramics. The crack growth velocity curves obtained for both ceramics were

shown in Fig.12. The diagram of the crack growth velocity (v) as a function of stress intensity factor ($K_I$) in logarithmic system was similar to typical v-$K_I$ curve with three characteristic regions (see Fig.1). The obtained curves of tested ceramics exhibit a different character.

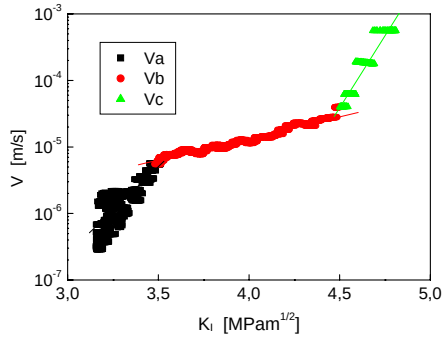


a

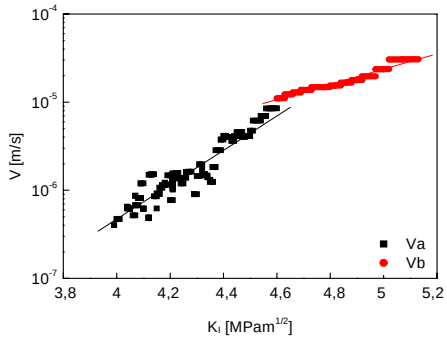


b

*Fig. 11. Crack growth velocity (v) versus stress-intensity factor ($K_I$) diagrams for: (a) $Al_2O_3$-10 wt% $ZrO_2$ (12 mol% $CeO_2$) ceramics and (b) $Al_2O_3$–10 wt% $ZrO_2$ with unstabilized $ZrO_2$.*

## 5. Conclusions

Fracture toughness determined according to conventional and indentation methods do not prove the significant difference in $K_{IC}$ values.

Alumina matrix composite with unstabilized zirconia characterizes itself the highest fracture toughness from among tested composites.

Carried out calculations and own measurements allow on the verification and evaluation of the usefulness of the proposed methods in determining the $K_{IC}$ for alumina matrix composites AMCs.

Indentation technique has certain advantages compared with the conventional method because the experimental procedure is straightforward, involving minimal specimen preparation and small amount of material.

The curves obtained from SCG as a function of crack growth velocity (v) versus stress intensity factor ($K_I$) in logarithmic system for tested ceramics exhibit a different character and it results from the different microstructure of the tested ceramics.

## References

[1] Sung R. Choi, Narottam P. Bansal, Strength, Fracture Toughness, and Slow Crack Growth of Zirconia/Alumina Composites at Elevated Temperature, Report NASA/TM—2003-212108
[2] http://www.ms.ornl.gov/programs/energyeff /cfcc/iof/chap24-6.pdf
[3] T. Fett, G. Martin , D. Muntz, J. Mater. Sci. **26**, 3320 (1991),
[4] D**.** Munz., T. Fett , Ceramics, Springer-Verlag, Berlin Heilderberg, (1999)
[5] De Aza A. H., Chvalier J., Fantozzi G., at all J. Am. Ceram. Soc. **86**(1), 115 (2003).
[6] M. Szutkowska, M. Boniecki, Proceedings of the 2002 World Congress on Powder Metallurgy and Particulate Materials PM2TEC 2002 [Advances in PM and Particulate Materials -2002] MPIF, July 16-21, Orlando, USA, (2002), part 6, p. 34. New York, Metal Powder Industries Federation, (2002).]
[7] T. Fett, Eng. Fract. Mech. **40**(5), 1194 (1994).
[8] M. Szutkowska, Proccedings: The Worldwide Congress of Materials and Manufacturing Engineering and Technology. Comment'2005. Gliwice-Wisła (2005), p.651
[9] J. Lankford**,** J. Mater. Sci. Lett. **1**, 493 (1982).
[10] K**.** Niihara et al.,Futher reply to "Comment on elastic/plastic indentation damage in ceramics: The median /radian crack system, Communications of the Amer. Ceram. Soc., C-116 (1982)
[11] M. Laugier , J. Mater. Sci. Lett., **6**, 355 (1987).
[12] G. Anstis**,** P. Chanticul. B.,Lawn., D. Marshall, J. Amer. Ceram.Soc., **64**(9), 533 (1981).
[13] K. Liang, G. Orange, G. Fantozzi**,** J. Mater. Sci**. 25,** 207 (1990).
[14] B. Lawn, E. Fuller**,** J. Mater. Sci.**10**, 2016 (1975).

*Corresponding author: szutkows@ios.krakow.pl